ACS APPLIED MATERIALS & INTERFACES

Research Article

www.acsami.org

Chemically Modified Graphene/Polyimide Composite Films Based on Utilization of Covalent Bonding and Oriented Distribution

Ting Huang, Renguo Lu, Chao Su, Hongna Wang, Zheng Guo, Pei Liu, Zhongyuan Huang, Haiming Chen, and Tongsheng Li*

State Key Laboratory of Molecular Engineering of Polymers, Department of Macromolecular Science, Fudan University, Shanghai, 200433, P. R. China

ABSTRACT: Herein, we have developed a rather simple composite fabrication approach to achieving molecular-level dispersion and planar orientation of chemically modified graphene (CMG) in the thermosetting polyimide (PI) matrix as well as realizing strong adhesion at the interfacial regions between reinforcing filler and matrix. The covalent adhesion of CMG to PI matrix and oriented distribution of CMG were carefully confirmed and analyzed by detailed investigations. Combination of covalent bonding and oriented distribution could enlarge the effectiveness of CMG in the matrix. Efficient stress transfer was found at the CMG/PI interfaces. Significant improvements in the mechanical performances, thermal stability, electrical conductivity, and hydrophobic behavior were achieved by addition of only a small amount of CMG. Furthermore, it is noteworthy that the hydrophilic-to-hydrophobic transition and the electrical percolation were observed at only 0.2 wt % CMG in this composite system. This facile methodology is believed to afford broad application potential in graphene-based polymer nanocomposites, especially other types of high-performance thermosetting systems.

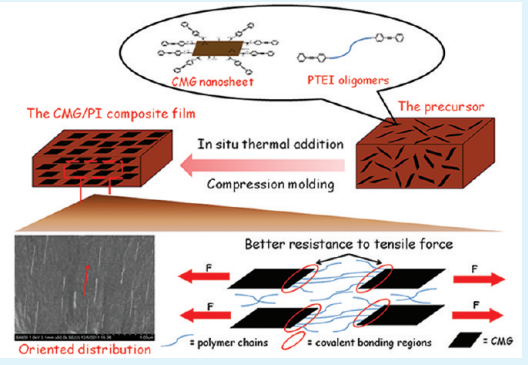

KEYWORDS: *polyimide, chemically modified graphene, efficient stress transfer, covalent bonding, oriented distribution, interfacial interactions*

1. INTRODUCTION

Chemically modified graphene (CMG), a two-dimensional (2D) and monoatomically thick building block composed of carbon allotrope functionalized with certain groups, has been considered as a versatile material of the 21st century.[1−3] Chemical modification of graphene oxide (GO), which is typically generated from wet oxidation of natural graphite flakes, has been a promising route to achieve mass production of CMG. Studies which utilize CMG to make high-performance materials have in part aroused a large surge in the field of various applications, such as field effect transistors, sensors, transparent conductive films, clean energy devices, and graphene/polymer composites.[4−7] However, the effectiveness of CMG is still far below what has been expected. Exploitation of the feasible fabrication of ideal and multifunctional graphene/polymer composites materials is still faced with numerous challenges, such as obtaining a homogeneous and oriented distribution of graphene in the matrix[8−10] and enhancing interfacial interactions between graphene and the matrix.[11−13]

Fortunately, both covalent functionalization and noncovalent functionalization methods have been proved to be effective means to improve the dispersibility of CMG in the polymer matrix.[14−16] For a high-quality composite, the homogeneous dispersion of CMG is a prerequisite but is not yet substantial. This is because poor stress transfer and interfacial slippage between two phases are induced due to weak van der Waals interactions based on the noncovalent functionalization method.[2−4] Note that the formation of covalent bonding between CMG and the matrix constitutes the strongest type of interfacial interactions; when properly executed, CMG could penetrate and become a part of the polymer matrix at a molecular level.[17] Furthermore, oriented distribution of nanoparticles within polymer nanocomposites is favorable for efficient stress transfer.[8] These two factors can provide substantial opportunities to attain ideal materials with high performances. To date, the incorporation of CMG into common engineering plastics has enhanced mechanical properties at extremely low loading.[12,18,19] However, only a few studies have been focused on the high-performance engineering plastics, such as polyphenylene sulfide, polyimide (PI), poly(*p*-benzamide), polyethersulfone, and polyetherimide.[1,2,4,5]

Aromatic PI is considered to be a typical well-established high-performance engineering plastic with a wide range of applications.[20−22] Up to now, more and more emphases have been laid on the pursuit of the PI-based materials with excellent performances because of practical demands from the microelectronics and aerospace industries.[23−25] Recently, although PI

Received: February 26, 2012
Accepted: April 11, 2012
Published: April 11, 2012

   dx.doi.org/10.1021/am3003439 | *ACS Appl. Mater. Interfaces* 2012, 4, 2699−2708

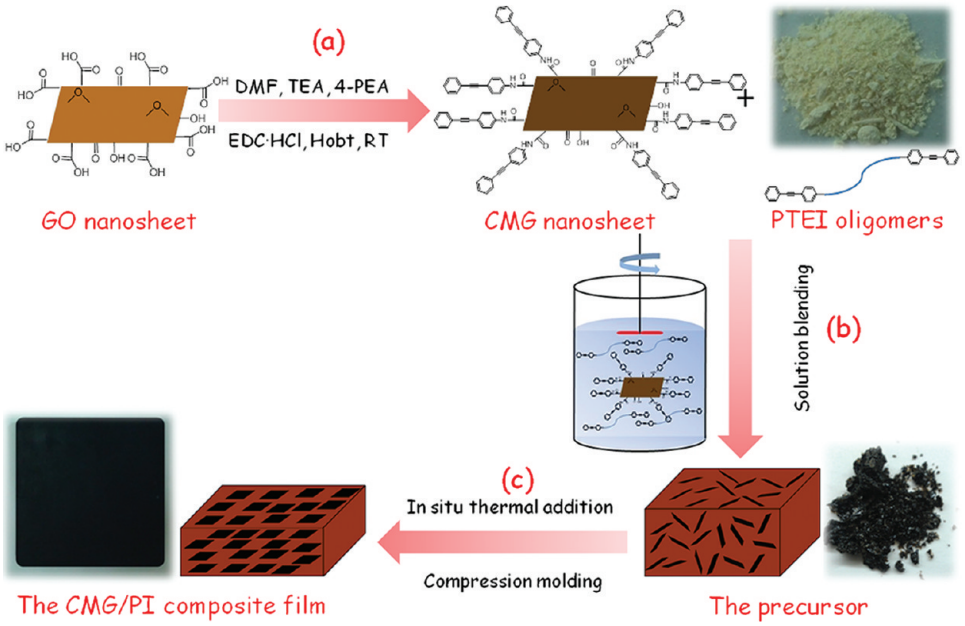

Figure 1. PE groups were covalently grafted on the edges of GO by (a) chemical modification of GO with 4-PEA. Preparation of the CMG/PI composite film via a two-stage process: (b) solution blending of CMG and PETI oligomers and (c) compression molding of the precusor.

composites employing GO were reported by some pioneering research, the actual improvement of the resulting PI composites was relatively lower than what we have expected.[26−29] In this regard, three significant issues have to be addressed. First, PI exhibits outstanding performances because of the cyclic imide structure in the polymer chains.[30] In the thermal imidization process, it is possible that an amide of the polyamic acid (PAA, the precursor of PI) could condense with a carboxylic acid of GO to form a linear imide linkage, which is thermally less stable than the cyclic imide structure. Second, the precursor cannot remain stable during the compounding process (high-speed mixing over long time). The decomposition of PAA will result in a lower molecular weight product with worse performances.[31] Third, high molecular weight polymers are difficult to graft to graphene because of notable steric hindrance effect of macromolecules.[29,32] It is highly desirable to search for another potential compounding strategy to overcome these drawbacks from the solution blending of CMG and PAA. In addition, hydrophobic CMG is more difficult to wet in comparison with graphite.[33,34] Herein, CMG also is expected as a preferred candidate to enhance hydrophobic behavior of PI.

On the basis of the above considerations, we have proposed an effective approach to fabricate high-performance CMG/PI composite films via a two-stage process: (i) solution blending of CMG functionalized with phenylethynyl (PE) groups and PE-terminated imide (PETI) oligomers and (ii) compression molding of the vacuum-dried precursors. During the hot-pressed procedure, covalent bonding regions were realized between CMG and PI matrix, due to the interfacial cross-linking via in situ thermal addition reactions of PE groups.[35,36] Moreover, the planar alignment of the resulting CMG nanosheets was achieved in response to the applied pressure. Additionally, the stability and relatively low calculated number-average molecular weight of PETI oligomers can be expected to overcome the decomposition and high steric hindrance effect, respectively. Efficient stress transfer was found between two phases, and the effectiveness of CMG was observed in this composite system. In order to in-depthly understand the related improvement mechanism, covalent bonding and oriented distribution were carefully analyzed and discussed by experimental results and Halpin−Tsai theoretical prediction.[37,38]

2. EXPERIMENTAL SECTION

2.1. Materials. Expandable graphite powders were provided from Yingtai Co. (Yangtai, China). Bisphenol-A dianhydride (BPADA) was purchased from Shanghai Research Institute of Synthetic Resins (Shanghai, China). 4-(Phenylethynyl)aniline (4-PEA) was purchased from Shanghai Apichemical Co., Ltd. (Shanghai, China). 1-Ethyl-3-(3-dimethylaminopropyl)carbodiimide hydrochloride (EDC·HCl) and 1-hydroxybenzotriazole (Hobt) were supplied from Aladdin reagent Co. (Shanghai, China). 4,4′-Oxidianiline (4,4′-ODA), ethanol, triethylamine (TEA), acetic anhydride, and *N*,*N*-dimethylformamide (DMF) were all reagent grade and provided by Sinopharm Group Chemical Reagent Co., Ltd. (Shanghai, China).

2.2. Preparation of CMG Functionalized with PE Groups. GO was synthesized from expandable graphite powders by the modified Hummers method, as described elsewhere.[39] The chemical modification of GO was carried out by a simple and facile amidation reaction (Figure 1a), which can be described as follows: 60 mg of GO powders were dispersed in 300 mL of DMF with the assistance of sonication at room temperature. Then, 0.6548 g (3.416 mmol) of EDC·HCl, 0.4614 g (3.414 mmol) of Hobt, 10 mL of TEA, and 0.6 g (3.105 mmol) of 4-PEA (excess amount) were added into the GO suspension, respectively. Afterward, the mixture was stirred at room temperature (RT) for 24 h under N_2. The powders, obtained from the matrix by vacuum filtration, were washed with excess DMF and deionized water successively four times, respectively. Finally, the solids were dried at 35 °C under vacuum overnight, yielding CMG. In the first and last cycle, the filtrates were carefully collected for Fourier transform infrared (FTIR) analysis.

2.3. Preparation of PTEI Oligomers and Precursors of CMG/PI Composite Films. PTEI oligomers based on BPADA, 4,4′-ODA, and 4-PEA with calculated number-average molecular weight of 5000 $g \cdot mol^{-1}$ were prepared by the conventional two-stage polymerization and imidization process, as reported elsewhere.[40] The precursors were fabricated by the solution blending method (Figure 1b). Briefly, 20 mg CMG powders were redispersed in 100 mL of DMF with the assistance of sonication for 2 h at RT. Then, 4 g PTEI oligomers were

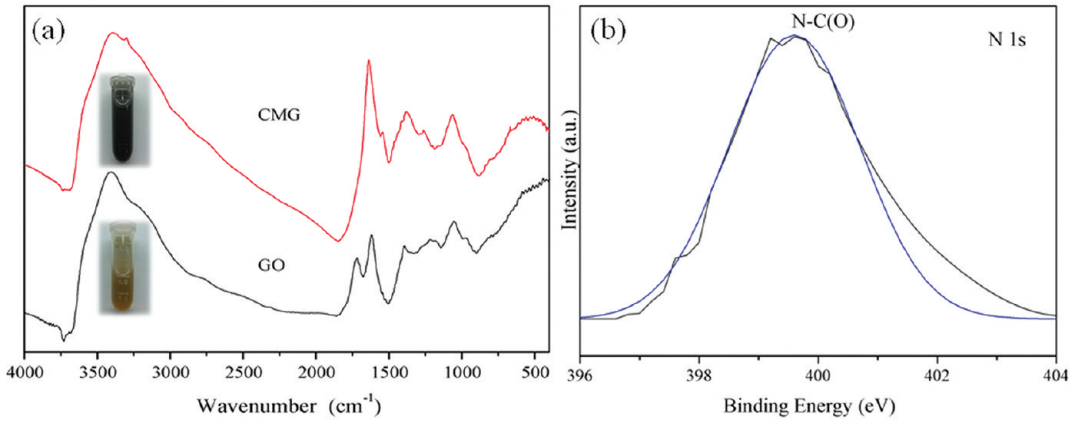

Figure 2. Structure characterization of as-prepared products: (a) FTIR spectra of GO and CMG, as well as photographs of their dispersions in DMF (inset), respectively; (b) N 1s XPS spectrum of CMG.

incorporated into the suspension. After sonication for 1 h and agitation at room temperature for another 12 h, the mixture was then separated out with 500 mL of ethanol (5:1 with respect to the amount of DMF used). The collected mixture was conducted by vacuum filtration and, afterward, vacuum-dried at 50 °C for 8 h, yielding the precursor of the resulting composite film (denoted as 0.5% CMG/PI) which has CMG loading of 0.5 wt %. For comparison, the precursors of the neat PI, 1 wt % GO/PI, and other CMG/PI composite films were fabricated in the same manner, respectively.

2.4. Preparation of CMG/PI Composite Films. All the film specimens were fabricated by the compression molding procedure. Typically, 1 g of the obtained precursors were first placed in a die and then heated gradually up to 260 °C at a rate of 4 °C·min^{-1}. Then, it was kept under a pressure of 1 to 2 MPa for 10 min. Several intermittent pressure relaxations (3 s each) were applied during the above procedure. The temperature continually increased to 320 °C; subsequently, the die was applied under a pressure of 5−10 MPa for 1 h at 320 °C. Afterward, the die was cooled under the applied pressure to less than 100 °C. Finally, the specimens were removed from the die to yield CMG/PI composite films with an average thickness of 120 ± 10 μm. The preparation process is briefly illustrated in Figure 1c. The resulting CMG/PI composite films were cut to desired sizes for various testing methods.

2.5. Characterization. Atomic force micrographs (AFM) of GO and CMG in DMF were obtained by a Digital Instruments Nano IV in tapping mode. Fourier transform infrared (FTIR) spectra were recorded on a Nicolet Nexus 470 spectrometer to characterize and confirm the chemical structure of GO and CMG, as well as the formation of covalent bonding between CMG and PI matrix. X-ray photoelectron spectroscopy (XPS) experiments were carried out on a RBD upgraded PHI-5000C ESCA system with Al Kα radiation (hv = 1486.6 eV). X-ray diffraction (XRD) patterns were acquired by a Panalytical X'pert diffractometer using Cu Kα radiation (λ = 0.154 nm) at an accelerating voltage of 40 kV and current of 40 mA. The glass transition temperature (T_g) was measured by a Netzsch 242 dynamic mechanical analyzer (DMA) in a tension mode. All the tests were run from 100 to 300 °C at a heating rate of 5 °C/min and conducted at a frequency of 1 Hz, vibration amplitude being set to 120 μm and static compressive stress of 4 N. The electrical conductivity of all the specimens was measured on a Keithley 2400 picoammeter using a standard four-probe method at RT. Thermogravimetric analyses (TGA) were carried out with a Perkin-Elmer thermal analyzer under nitrogen flow at a heating rate of 20 °C·min^{-1}. Contact angle measurements were measured on an OCA 40Micro contact angle meter from Dataphysics Instruments GmbH. Mechanical properties were evaluated using a universal testing machine (CMT-4102, Sans Co., China) for dumbbell-type specimens, according to ISO 527-3:1995 standard. The data reported here represent the average of five tests. Scanning electron microscopy (SEM) images of the tensile-fractured surfaces were observed on a Tescan 5136 MM SEM. Thin sections for field emission scanning electron microscopy (FESEM) observations were cut from the as-prepared composite films under cryogenic conditions using a Leica ultramicrotome with a diamond knife, and FESEM images were conducted on a Hitachi S-4800 FESEM to observe the distribution of CMG in the PI matrix.

3. RESULTS AND DISCUSSION

3.1. Characterization of CMG. The dispersibility of chemically modified GO (CMG) in common solvents is a crucial role to obtain homogeneous polymer composites by solution blending. To guarantee the retention of the dispersibility of CMG in DMF, oxygen-containing functional groups of GO except carboxylic acid groups should be avoided to react as much as possible during the chemical modification. The proposed mechanism for chemical modification of GO is that an amide linkage is formed between the aromatic amino of 4-PEA and the edge-carboxylic acid groups of GO with the aid of EDC·HCl and Hobt as coupling agents.[15,41,42] As illustrated in Figure 2a, there are some characteristic GO absorptions at 1730 and 1620 cm^{-1}, which are attributed to C═O stretching vibration of carboxyl and C═C stretching vibration of aromatic ring, respectively. By the incorporation of 4-PEA, the band of GO at 1730 cm^{-1} disappears while a new band at 1645 cm^{-1} assigned to C═O stretching vibration of amide carbonyl is observed. Besides, the bands at 3300 cm^{-1} (N−H stretching vibration of amide) and 1545 cm^{-1} (N−H bending vibration of amide) appear in the spectrum.[43] These results support the success of chemical modification of GO by the amidation reaction. As expected, the bands at 1065 cm^{-1} (C−O−C in epoxide groups) and 3300−3500 cm^{-1} (−OH stretching vibration of hydroxyl groups) still remain in the spectrum of CMG, indicating that other oxygen-containing functional groups such as epoxide and hydroxyl groups were retained on the surface of CMG. XPS results also suggest the covalent adhesion of 4-PEA to GO through the amide bonding formation (Figure 2b). Thus, PE groups of 4-PEA can be grafted simultaneously on the edges of CMG due to the location of the amide bonding.

The collected filtrates, including the first filtrate and last filtrate, were analyzed by FTIR. As illustrated in Figure 3, the first filtrate as well as 4-PEA exhibits the characteristic absorption at around 2213 cm^{-1}, which is assigned to the stretching vibration of ethynyl C≡C. The existence of PE groups in the filtrate after reactions provides distinct evidence

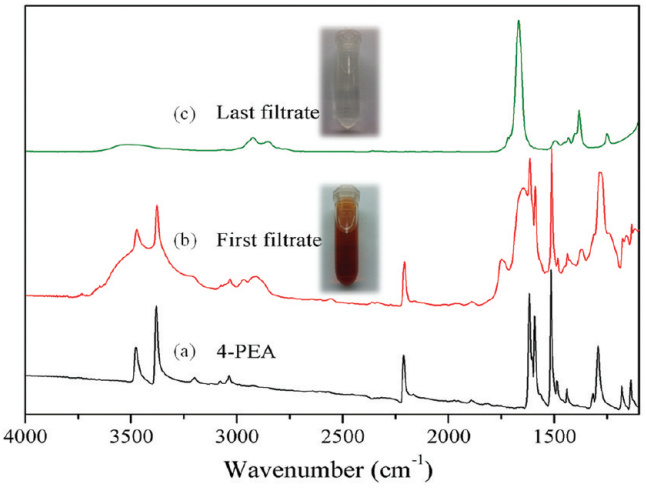

Figure 3. FTIR spectra of (a) 4-PEA, (b) first filtrate, and (c) last filtrate, as well as photographs of the first filtrate and last filtrate (inset), respectively.

that cross-linkable groups (PE groups) remain unreacted during the amidation reaction. It indirectly demonstrates that PE groups remain chemically intact on the edges of CMG. However, no characteristic absorption (C≡C 2213 cm^{-1}) is observed in the last filtrate. Compared to the first filtrate, the last filtrate appears to be colorless. According to the above results, it is reasonably believed that the resulting CMG free of 4-PEA has been successfully prepared.

In order to illustrate the complete exfoliation of CMG in DMF, we obtained the AFM images of GO and CMG redispersed in DMF under tapping mode (Figure 4). From the cross-section analysis, it is found that CMG is typically a few to several hundred nanometers in size and has a height of around 0.9 nm, matching well with the reported thickness of CMG.[1−5] It should be noted that the thickness of CMG is slightly higher than that of GO (0.77 nm), which can be due to the grafting of 4-PEA.[43]

Generally, the common way to prepare graphene/polymer composites is utilizing homogeneous GO dispersion in organic solvents.[2−5,43] As previously reported in the literature,[44] hydrophilic GO cannot be evenly dispersed in certain organic solvents, such as dimethyl sulfoxide (DMSO) and cyclohexane. Due to the insolubility of graphene and its derivatives, only the dispersibility of CMG was tested in common organic solvents, at 0.5 mg/mL loading (Figure 5). The CMG turns out to be homogeneously dispersed in dimethylacetamide (DMAc), DMF, DMSO, dioxane, and cyclohexane. It affords more approaches to prepare other polymer composites except for PI composites. On the contrary, CMG agglomerates in *N*-methyl-2-pyrrolidone (NMP). These results are mainly ascribed to the introduction of nonpolar benzene groups to GO through the amidation reaction.

3.2. Characterization of CMG/PI Composite Films. Since as-prepared CMG can be dispersed in a wide variety of organic media as individual sheets, it allows their homogeneous incorporation into polymer matrixes. The photograph of the resulting PI composite films (dumbbell-type, for mechanical tests) is displayed in Figure 6a. Apparently, all the CMG/PI composite films show homogeneous appearance by visual inspection, indicating uniform dispersion of CMG in the PI matrix.

To further confirm the absence of CMG aggregation in the polymer matrix, the XRD patterns of GO, CMG, neat PI, and CMG/PI specimens are presented in Figure 6b. Compared to the strong diffraction peak of GO located at 11.4° (corresponding to interlayer spacing of about 0.77 nm), that of CMG is slightly shifted to a lower 2θ Bragg angle (9.8°), indicating the incorporation of 4-PEA enlarges intragallery space.[45] However, the XRD patterns of CMG/PI composite films present neither graphite layer structure peak at 26° nor CMG peak at 9.8°. The XRD results demonstrate the vanishment of the stacking and regular structure of CMG, supporting further evidence of the complete exfoliation of CMG.[46] As suggested by Ramanathan et al.,[47] the dispersion of CMG nanosheets in the PI matrix is close to single-sheet level.

As reported in recent literature,[2,4,5,13] covalent bonding affords strong interfacial interactions, as well as good compatibility between CMG and the matrix, maximizing the extraordinary performance of CMG. To confirm the

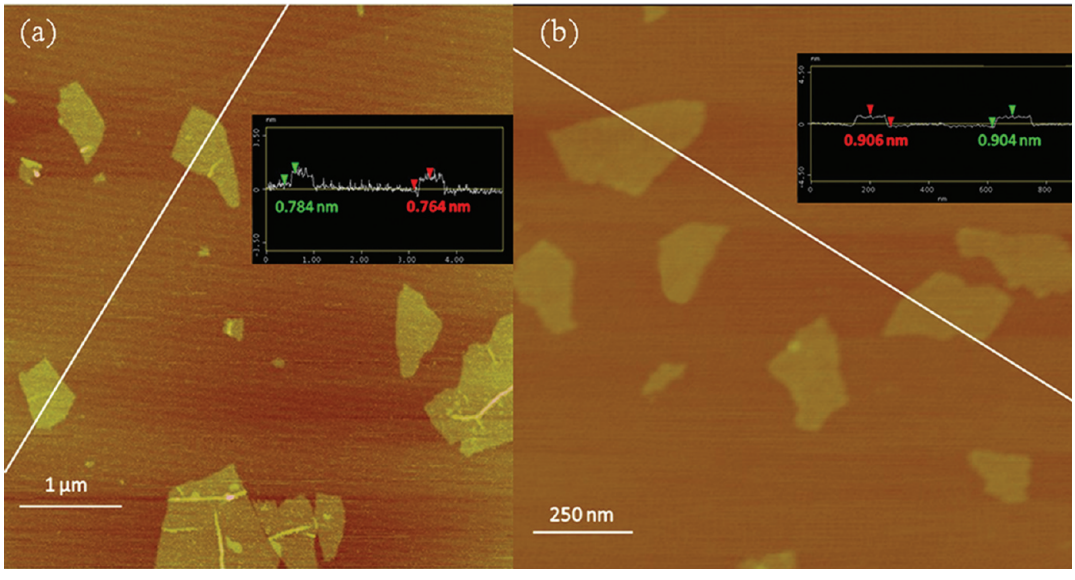

Figure 4. Typical tapping mode AFM images of (a) GO and (b) CMG, as well as their cross-section analyses (inset), respectively.

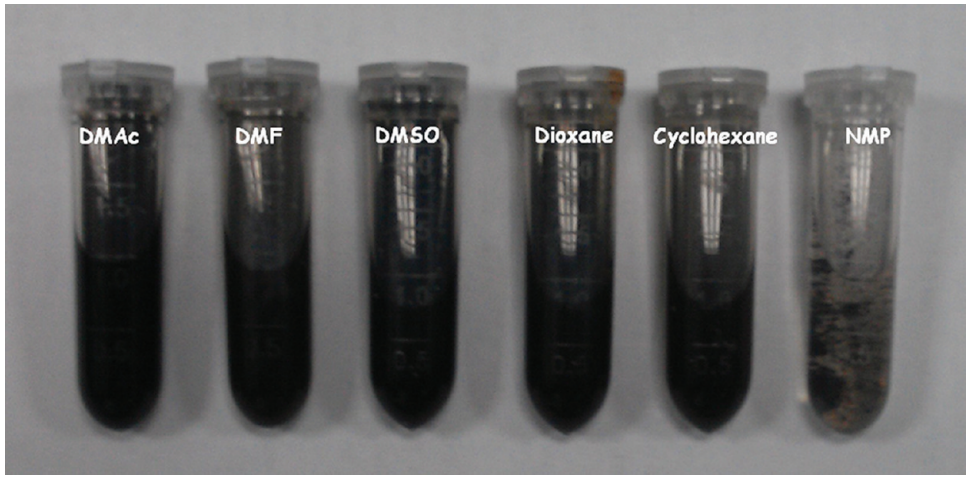

Figure 5. Dispersibility of CMG in common organic solvents.

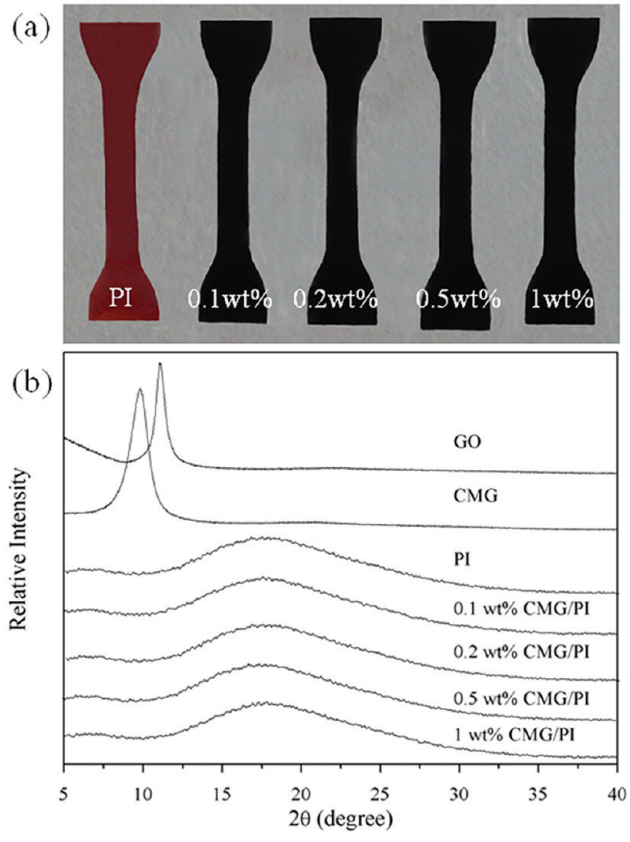

Figure 6. (a) Appearance of dumbbell-type specimens of the neat PI and CMG/PI composite films. (b) XRD patterns of GO, CMG, neat PI, and CMG/PI composite films.

implementation of the covalent adhesion at the CMG/PI interfaces, Figure 7 illustrates FTIR spectra of the precursor and typical CMG/PI composite film. It is found that the absorption band of the precursor at around 2213 cm^{-1} is ascribed to ethynyl C≡C while the absorption band in the CMG/PI composite film is absent. Obviously, it indicates that PE groups in the precursor (CMG/PTEI powders) have undergone a complex thermal addition reaction.[40,48] It should be noted that PTEI oligomers have been adopted and PE groups have been grafted onto the CMG, as well as the fact that the dispersion of CMG nanosheets in the matrix is close to single-sheet level.

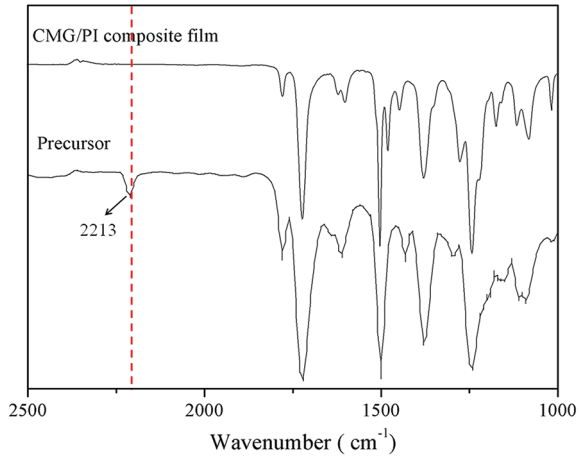

Figure 7. FTIR spectra of the precursor and typical CMG/PI composite film.

Therefore, the in situ thermal addition step contains (a) interchain and (b) interfacial cross-linking, providing interfacial covalent cross-links between CMG and PI matrix under only a small amount of CMG (≤1 wt %). The strong interfacial interactions are developed in the two-phase matrix, and the dispersibility of CMG in the matrix can be improved as well.[49] As suggested by Feng et al. or Li et al.,[26,45,50] the thermal reduction of CMG such as dehydration and deoxygenation can take place during the compression-molding condition since higher temperature and more time (320 °C for 1 h) were adopted compared to that reported in the literature, and this can reduce the defect sites of CMG and simultaneously make CMG more hydrophobic and electrically conductive, providing an ideal filler for polymer matrix.

Given the existence of covalent bonding at the CMG-PI interfaces and homogeneous CMG dispersion, one would expect a substantial enhancement in the T_g of the resulting composite films with the addition of CMG. Representative results of loss factor (tan δ) as a function of temperature (T) for all the specimens are presented in Figure 8, from which the T_g is extracted in terms of the peak termperature of tan $\delta \sim T$ cure. The T_g of the CMG/PI composite films displays a clear increasing trend with increasing CMG concentration, showing the greatest value at 1 wt %. It is reasonable that such good dispersion and strong interfacial interactions contribute to

dx.doi.org/10.1021/am3003439 | ACS Appl. Mater. Interfaces 2012, 4, 2699−2708

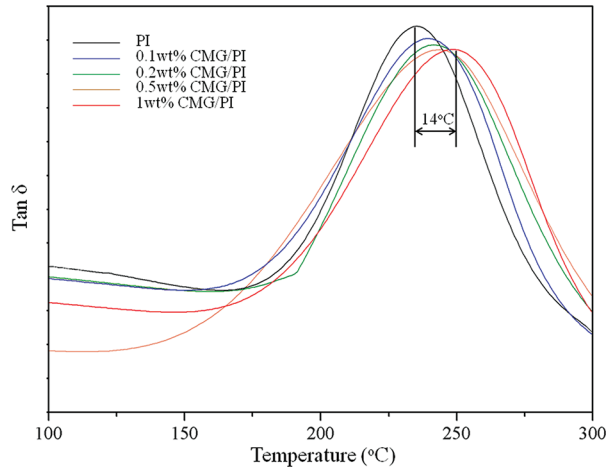

Figure 8. Changes of tan δ of the neat PI and CMG/PI composite films with increasing temperature.

enhancing the T_g in the CMG/PI composite system. Note that the increase of 14 °C in T_g in this composite system is relatively high compared to the reported value for the expanded graphite/PI composite system,[51] indicating a stronger confinement effect due to covalent adhesion between CMG and PI matrix. With the increase of CMG in the PI composite films, the number of confined chains increases and therefore the improvement in T_g is a natural result.

Given the excellent elastic modulus and intrinsic strength of CMG,[2,3] it can be expected that mechanical performances of the CMG/PI composite films would be improved remarkably by large aspect ratio of CMG, molecular-level dispersion of CMG in the PI matrix, and strong interfacial interactions. Relationships of mechanical performances with filler loading are illustrated in Figure 9a. Obviously, the mechanical properties of the CMG/PI composite films are greatly enhanced compared to that of the neat PI. For instance, although the intrinsic tensile strength of the neat PI is relatively high (~102 MPa), it should be noted that the tensile strength significantly increases by 30% with only 1 wt % (0.64 vol%) CMG incorporated (Figure 9a), and the Young's modulus correspondingly increases by 46% (Figure 10). However, the elongation at break presents a slightly downward trend with increasing CMG content. Due to the confinement effect, the immobilization of some segments on the CMG may influence the elongation at break of final products. Fortunately, the resulting CMG/PI composite films still maintain relatively high elongation at break, indicating that the incorporation of a small quantity of CMG cannot hinder the flexibility of the resulting composite films (Figure 9b).

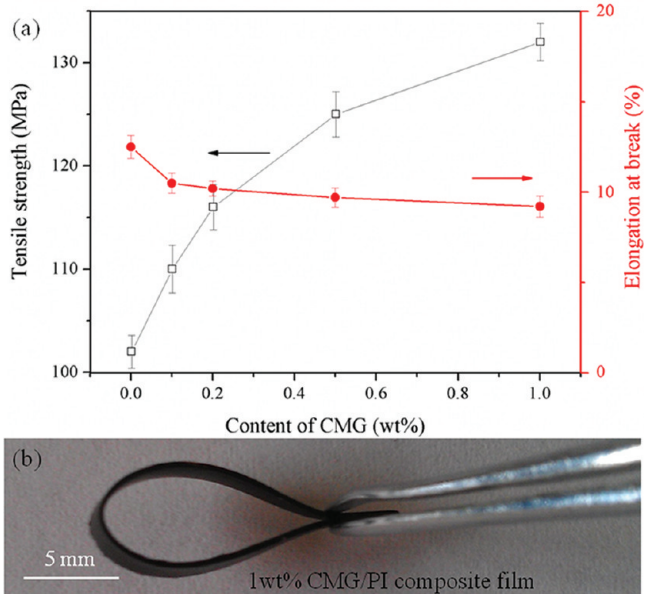

Figure 9. (a) Relationships of tensile strength and elongation at break with various CMG concentrations. (b) A typical photographic image illustrates that the 1 wt % CMG/PI composite film still retains flexibility well.

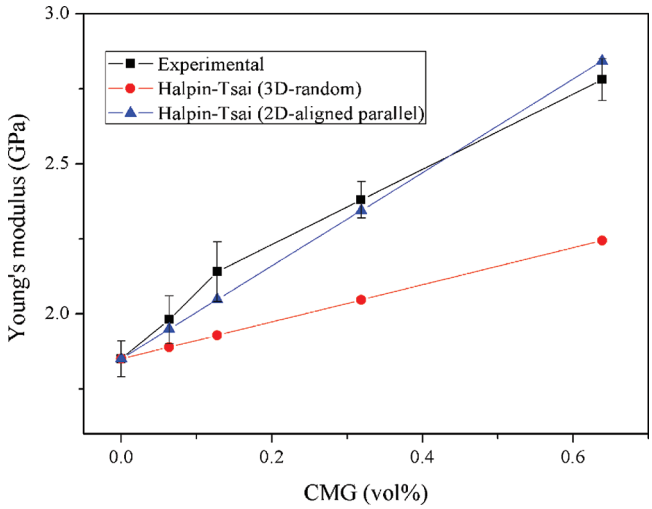

Figure 10. Young's modulus of the experimental and Halpin–Tsai theoretical model. Two hypotheses were proposed as follows: 3D-random and 2D-aligned parallel distributions of CMG in the PI matrix, respectively.

In an attempt to explore the improvement mechanism, further discussion on the issue of the CMG distribution is warranted. The Halpin–Tsai model is widely used for predicting the modulus of unidirectional or randomly distributed filler-reinforced polymer composite.[35,36,43] Hence, it has been applied to simulate the Young's modulus of CMG/PI composite films in this work. The Young's modulus of the resulting composite films was calculated according to the modified Halpin–Tsai equation, as follows:

$$E_c = \left[\frac{3}{8}\cdot\frac{1+(2L_g/3T_g)\eta_L V_g}{1-\eta_L V_g} + \frac{5}{8}\cdot\frac{1+2\eta_T V_g}{1-\eta_T V_g}\right]E_p \quad (1)$$

$$E_{aligned} = \left[\frac{1+(2L_g/3T_g)\eta_L V_g}{1-\eta_L V_g}\right]E_p \quad (2)$$

$$\eta_L = \frac{(E_g/E_p)-1}{E_g/E_p + 2L_g/3T_g} \quad (3)$$

$$\eta_T = \frac{(E_g/E_p)-1}{E_g/E_p + 2} \quad (4)$$

dx.doi.org/10.1021/am3003439 | ACS Appl. Mater. Interfaces 2012, 4, 2699–2708

$$V_g = \frac{W_g \rho_p}{W_g \rho_p + (1 - W_g)\rho_g} \quad (5)$$

Here, E_c and $E_{aligned}$ refer to the Young's modulus of the composite films, randomly oriented and aligned parallel to the surface of the specimen, respectively. L_g, T_g, and V_g refer to the length, thickness, and volume fraction of CMG in the PI matrix. The Young's modulus of CMG (E_g) was previously measured as around 0.25 TPa,[52] and that of the pristine PI (E_p) is 1.85 GPa according to the experimental result. The average length and thickness of CMG are around 300 and 0.9 nm, on the basis of the AFM analysis, respectively. The density of the pristine PI (ρ_p) is 1.4 g·cm^{-3}, and that of CMG (ρ_g) is 2.2 g·cm^{-3}.[1−5] Using these values into eqs 1−5, the Young's modulus of the resulting composite film was calculated under two presupposed distributions of CMG. As shown in Figure 10, one can see that the theoretical simulation for the 2D-aligned parallel distribution shows good consistency with the experimental results collected from the resulting composite films, which apparently indicates that CMG is aligned preferentially parallel to the surface. This planar orientation can ensure efficient stress transfer at the CMG/PI interfaces via covalent interactions.[46] However, the evidence is not sufficient; the distribution of CMG demands further investigation.

Figure 11 provides direct evidence of the distribution of CMG within the PI matrix. As-prepared CMG is not only homogeneously dispersed in the matrix but also well aligned along the surface (indicated by a red arrow). Interestingly, it can be seen that CMG is embedded into host polymer with its flake-like morphology remaining intact, indicating that CMG intimately interacts with the matrix. It shows another evidence of the strong interfacial adhesion between CMG and PI matrix, affording efficient stress transfer. Although the occurrence of volatiles (H_2O and other oxygen-containing byproducts) evolved during the thermal reduction, it appears that the intermittent pressure relaxations can overcome the negative effects of volatiles because compacted CMG/PI composites without any defects are observed (Figure 11). The formation of the oriented distribution of CMG within the PI matrix could be explained by the simplified schematic diagram, as illustrated in Figure 12a. Because melting PTEI oligomers have a low- and wide-viscosity region,[48] CMG can relatively freely stand in the melting precursor before the thermal addition reactions of PE groups. Compared with the traditional solution casting method, the hot-pressed procedure can provide extra uniform vertical stress, inducing CMG with large aspect ratio to be planarly oriented along the film surface direction. Additionally, the thickness of the resulting composite films is about 120 μm whereas the lateral size of CMG is several hundred nanometers,

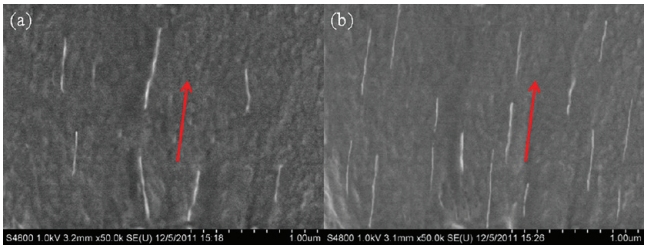

Figure 11. Structure characterization of the oriented distribution of (a) 0.5 wt % CMG and (b) 1 wt % CMG in the PI matrix, respectively (FESEM images: side view).

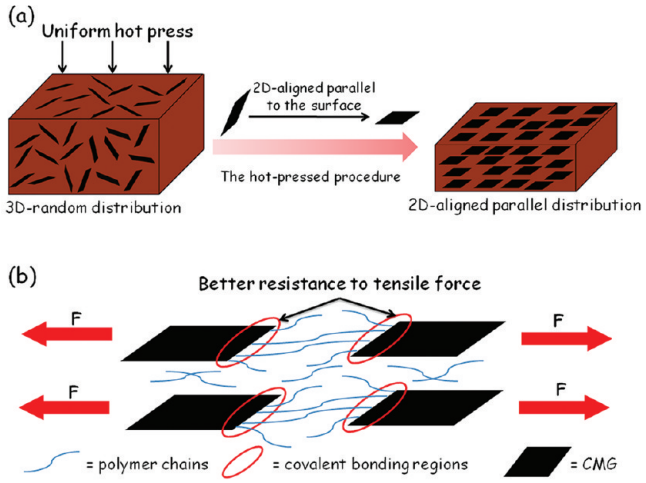

Figure 12. (a) Simplified schematic description of the oriented distribution mechanism of CMG in the PI matrix. (b) Typical proposed model for the enhanced mechanical properties of the CMG/PI composite films.

and CMG tends to be spontaneously aligned along the film surface direction.[26]

On the basis of the above investigations, covalent bonding and oriented distribution should be further addressed as two critical factors in the analysis for the improvement of mechanical properties. The enhanced mechanical properties observed from the CMG/PI composite film is consistent with the typical interpretation model, as shown in Figure 12b. Covalent bonding of CMG to PI matrix provides strong interfacial interactions throughout the composite films. Due to the facts of planar orientation of CMG and the location of PE groups, covalent bonding regions are located predominantly on the edges of CMG. For graphene/polymer composites, the reinforcement effect of CMG to polymer hosts largely depends on the efficiency of stress transfer at the interfaces.[46] On tensile loading, covalent bonding regions, adequately utilizing the advantages of covalent bonding and oriented distribution, can enable efficient stress transfer across the CMG/PI interfaces, thus resisting the tensile force better. On the whole, it is believed that CMG acts as an important role as a connecting bridge throughout the PI matrix because of oriented distribution of filler.[53] Actually, it can effectively prevent the CMG/PI composite films from fracturing under mechanical deformation. In addition, the good dispersion of CMG in PI matrix (Figure 11) can decrease the stress concentration, afford more even stress distribution, and increase the interfacial areas for efficient stress transfer, thus improving properties of the PI composite films.[54,55]

As supplements, the tensile fracture surfaces of the neat PI and CMG/PI composite films were investigated. As shown in Figure 13, the fracture surface of the neat PI film presents a relatively smooth and flat surface while those of the CMG/PI composite films show rather rough surfaces. It may be ascribed to the strong interfacial interactions between CMG and PI matrix. Note that layered structures aligned parallel to the surface are presented on the fracture surfaces of the CMG/PI composite films, especially for higher loading of CMG. Due to the planar orientation of CMG, it is believed that the resin-coated CMG is encapsulated into a layered structure in the PI matrix. When the addition of CMG is up to the critical point,

dx.doi.org/10.1021/am3003439 | ACS Appl. Mater. Interfaces 2012, 4, 2699−2708

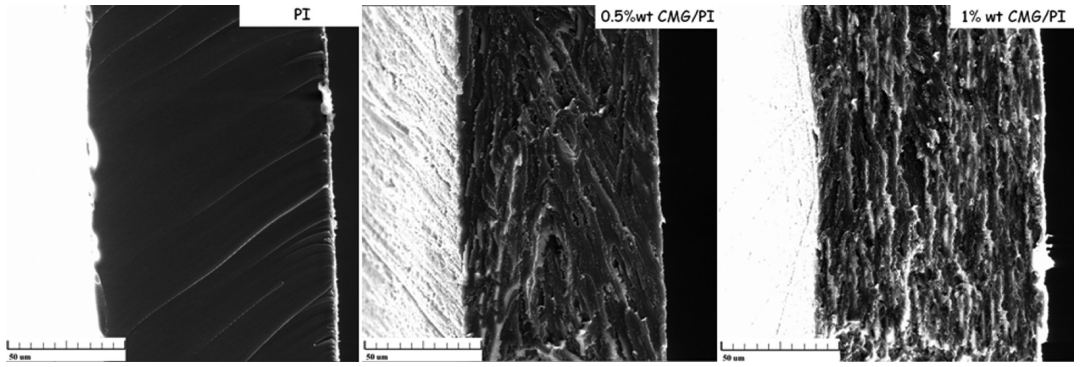

Figure 13. SEM micrographs of the fracture surfaces of the neat PI and CMG/PI composite films (magnification: 1000).

the resulting composite films would spontaneously lead to layered-structure fractures upon the external tensile force.[56,57]

In hot pursuit of multifunctional composite films, hydrophobic behavior of materials is a crucial performance index. As reported by Wang et al.,[33] the average water contact angle of chemically reduced GO is near 127°. Consequently, water contact angle of the resulting composite films requires further investigations. As shown in Figure 14, this parameter has a

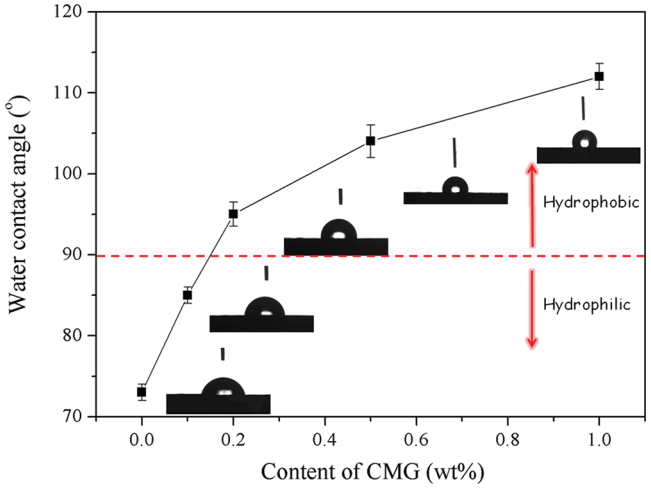

Figure 14. Average water contact angle measured by the droplet and typical photographs of the water contact angle on the surfaces of the specimens (inset).

remarkable upward trend with the increase of CMG. A 55% increase in the water contact angle is achieved by addition of only 1 wt % CMG. Note that the wetting behavior of the neat PI film is altered with only a small amount (0.2 wt %) of CMG incorporated. The reasons for such an obvious improvement in hydrophobic behavior should be ascribed as follows: (a) carboxylic acid groups are reacted off and simultaneously nonpolar benzene groups are linked by chemical modification of GO; as well as CMG has undergone the thermal reduction during the compression-molding procedure, which all improve hydrophobic behavior of CMG; (b) the hydrophobic effect of CMG comes primarily from a 2D-monatomic thick surface; the location of covalent bonding regions on the edges of CMG may maximize the utilization of hydrophobic effect; (c) the homogeneous and planar orientation of CMG with large aspect ratio affords high efficient enhancement at low filler loading. It is believed that the successful application of hydrophobic effect of CMG reveals that CMG is promising to be a hydrophobic nanoscale filler in the polymer composite materials.

The conductive behavior of graphene aroused the investigation on the effect of CMG on the conductivity of the resulting CMG/PI composite films. The CMG/PI composite films may conduct electricity because of partial thermal reduction occurring in the compression molding procedure. Therefore the electrical conductivity measurement was performed. As shown in Figure 15, it exhibits a sharp

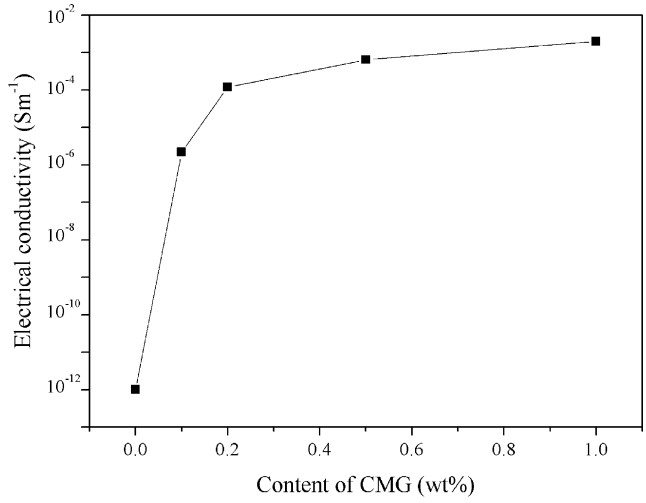

Figure 15. Electrical conductivity of the neat PI and CMG/PI composite films.

improvement in the conductivity of the CMG/PI composite films when the content of CMG approaches 0.2 wt %, reflecting effective thermal reduction. The values of the conductivity for the CMG/PI composite films are above the antistatic criterion of 10^{-6} Sm^{-1} and continue to increase until the filler content increases to 1 wt %. The CMG/PI composite films hold an electrical percolation threshold (about 0.2 wt %). Such a rather low electrical percolation threshold may be explained by the homogeneous and planar orientation of CMG in PI matrix and effective thermal reduction as well as the effective exfoliation of CMG with extraordinarily large specific surface area. It is interesting to note that the conductivity of the CMG/PI composite system is higher than that previously reported in the literature,[27] and this may be caused by much higher reduction degree during higher temperature thermal treatment and planar orientation of CMG in the PI matrix.

As a kind of high-engineering plastic, thermal stability is another key performance for PI composite films. Figure 16

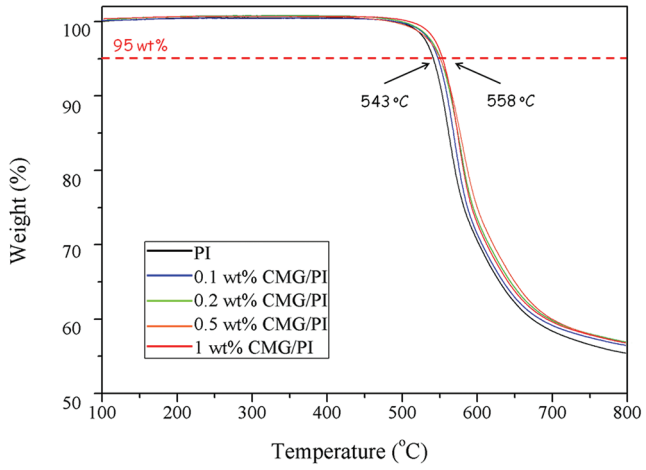

Figure 16. TGA thermograms of the neat PI and CMG/PI composite films.

illustrates the TGA traces of the neat PI and CMG/PI composite films. It is found that the temperature for 5% weight loss of the resulting composite films exhibits a respectable increase (~15 °C) by addition of 1 wt % CMG. The implementation of covalent adhesion between two phases affords good compatibility and even more uniform integration, which both can take advantage of the thermal stability of CMG. As Cao and co-workers suggested,[11] the homogeneous and planar orientation of CMG in the matrix also utilizes thermal stability of fillers more efficiently. Moreover, CMG with large aspect ratio brings out the so-called "tortuous path" effect, which acts as barriers to prevent the permeation of oxygen and the escape of volatile degradation products and also char formation.[58,59] Thereby, the improvement in thermal stability of composite films is achieved.

To further illustrate the effect of chemical modification of GO, a systematical comparison has been performed between 1 wt % CMG/PI and 1 wt % GO/PI composite films. As expected, one can see that CMG can improve properties of the resulting PI composite films better, except for the elongation at break (Table 1), indicating that the interfacial covalent bonding can utilize the effectiveness of CMG more efficiently in the matrix due to the strong interfacial interactions. Fortunately, 1 wt % CMG/PI composite film still retains a thermalplastic-like flexibility (Figure 9b).

Table 1. Data Based on Properties of 1 wt % CMG/PI and 1 wt % GO/PI Composite Films

specimens	1 wt % CMG/PI composite films	1 wt % GO/PI composite films
tensile strength (MPa)	132	121
Young's modulus (GPa)	2.78	2.48
elongation at break (%)	9.2	10.1
T_g (°C)	249	235
T_5[a] (°C)	558	546
electrical conductivity (Sm^{-1})	2.1×10^{-3}	9.8×10^{-4}

[a]T_5: the temperature at 5 wt % of weight loss was recorded by TGA with a heating rate of 20 °C/min under N_2 atmosphere.

4. CONCLUSIONS

In summary, we have developed a novel and facile approach for the fabrication of high-performance CMG/PI composite films. The cross-linkable groups (PE groups) are introduced into both GO and oligomers, and this can form interfacial covalent bonding via the self-reaction of cross-linkable groups. The implementation of covalent bonding regions at the CMG/PI interfaces strengthens interfacial interactions and simultaneously improves the dispersibility of CMG. Both experimental results and theoretical simulation demonstrate the planar orientation of CMG in the PI matrix. Efficient stress transfer across the interfaces, together with enhanced performances of the PI composite films, is achieved by taking advantage of covalent adhesion and oriented distribution. The 1 wt % CMG/PI composite film exhibits a 30% increase in tensile strength and a 46% raise in Young's modulus. The hydrophilic-to-hydrophobic transition and the electrical percolation threshold are observed at only 0.2 wt % CMG in this composite system. This work presented herein greatly broadens the application scope of CMG and will be of interest to communities in polymer matrix composites, graphene-based materials for nanoelectronics, and smart materials.

AUTHOR INFORMATION

Corresponding Author

*Fax: +86-21-51630401. E-mail: lits@fudan.edu.cn.

Notes

The authors declare no competing financial interest.

REFERENCES

(1) Dreyer, D. R.; Park, S.; Bielawski, C. W.; Ruoff, R. S. *Chem. Soc. Rev.* **2010**, *39*, 228−240.
(2) Kim, H.; Abdala, A. A.; Macosko, C. W. *Macromolecules* **2010**, *43*, 6515−6530.
(3) Stankovich, S.; Dikin, D. A.; Dommett, G. H. B.; Kohlhass, K. M.; Zimney, E. J.; Stach, E. A.; Piner, R. D.; Nguyen, S. T.; Ruoff, R. S. *Nature* **2006**, *442*, 282−286.
(4) Zhu, Y. W.; Murali, S. T.; Cai, W. W.; Li, X. S.; Suk, J. W.; Potts, J. R.; Ruoff, R. S. *Adv. Mater.* **2010**, *22*, 3906−3924.
(5) Singh, V.; Joung, D.; Zhai, L.; Das, S.; Khondaker, S. I.; Seal, S. *Prog. Mater. Sci.* **2011**, *56*, 1178−1271.
(6) Li, X.; Wang, X.; Zhang, L.; Lee, S.; Dai, H. *Science* **2008**, *319*, 1229.
(7) Pan, Y. Z.; Bao, H. Q.; Sahoo, N. G.; Wu, T. F.; Li, L. *Adv. Funct. Mater.* **2011**, *21*, 2754−2763.
(8) Gorrasi, G.; Lieto, R. D.; Patimo, G.; Pasquable, S. D.; Sorrentino, A. *Polymer* **2011**, *52*, 1124−1132.
(9) Bin, Y.; Kitanaka, M.; Zhu, D.; Matsuo, M. *Macromolecules* **2003**, *36*, 6213−6219.
(10) Uddin, A. J.; Araki, J.; Gotoh, Y. *Biomacromolecules* **2011**, *12*, 617−624.
(11) Cao, Y. W.; Lai, Z. L.; Feng, J. C.; Wu, P. Y. *J. Mater. Chem.* **2011**, *21*, 9271−9278.
(12) Shen, B.; Zhai, W. T.; Chen, C.; Lu, D. D.; Wang, J.; Zheng, W. G. *ACS Appl. Mater. Interfaces* **2011**, *3*, 3103−3109.
(13) Fang, M.; Wang, K. G.; Lu, H. B.; Yang, Y. L.; Nutt, S. *J. Mater. Chem.* **2009**, *19*, 7098−7105.
(14) Yang, H. F.; Shan, C. S.; Li, F. H.; Han, D. X.; Zhang, Q. X.; Niu, L. *Chem. Commun.* **2009**, *26*, 3880−3882.
(15) Pan, Y. Z.; Bao, H. Q.; Li, L. *ACS Appl. Mater. Interfaces* **2011**, *3*, 4819−4830.
(16) Das, S.; Wajid, A. S.; Shelburne, J. L.; Liao, Y. C.; Green, M. J. *ACS Appl. Mater. Interfaces* **2011**, *3*, 1844−1851.
(17) Feng, R. C.; Zhou, W.; Guan, G. H.; Li, C. C.; Zhang, D.; Xiao, Y. N.; Zheng, L. C.; Zhu, W. X. *J. Mater. Chem.* **2012**, *22*, 3982−3989.

(18) Rafiq, R.; Cai, D. Y.; Jin, J.; Song, M. *Carbon* **2010**, *48*, 4309−4314.
(19) Goncalves, G.; Marques, P.; Barros-Timmons, A.; Bdkin, I.; Singh, M. K.; Emami, N.; Grácio, J. *J. Mater. Chem.* **2010**, *20*, 9927−9934.
(20) Bin, Y. Z.; Oishi, K.; Koganemaru, A.; Zhu, D.; Matsuo, M. *Carbon* **2005**, *43*, 1617−1627.
(21) Ge, J. J.; Zhang, D.; Li, Q.; Hou, H. Q.; Graham, M. J.; Dai, L. M.; Harris, F. W.; Cheng, S. Z. D. *J. Am. Chem. Soc.* **2005**, *127*, 9984−9985.
(22) Gooding, J. J. *Electrochim. Acta* **2005**, *50*, 3049−3060.
(23) Kakade, B.; Mehta, R.; Durge, A.; Kulkarni, S.; Pillai, V. *Nano Lett.* **2008**, *8*, 2693−2696.
(24) Chuang, M. J. *Surf. Coat. Technol.* **2009**, *203*, 3527−3532.
(25) Tagawa, M.; Maeda, K. I.; Kajita, T.; Yokota, K.; Akamatsu, K.; Nawafune, H. *Langmuir* **2007**, *23*, 11351−11354.
(26) Chen, D.; Zhu, H.; Liu, T. X. *ACS Appl. Mater. Interfaces* **2010**, *2*, 3702−3708.
(27) Luong, N. D.; Hippi, U.; Korhonen, J. T.; Soininen, A. J.; Ruokolainen, J.; Johansson, L. S.; Nam, J. D.; Nam, L. D.; Sinh, L. H.; Seppälä, J. *Polymer* **2011**, *52*, 5237−5242.
(28) Kim, G. Y.; Choi, M. C.; Lee, D.; Ha, C. S. *Macromol. Mater. Eng.* **2012**, *297*, 303−311.
(29) Liu, H.; Li, Y. Q.; Wang, T. M.; Wang, Q. H. *J. Mater. Sci.* **2011**, *47*, 1867−1874.
(30) Sroog, C. E. *J. Polym. Sci.: Macromol. Rev.* **1976**, *11*, 161−208.
(31) Bryant, R. G. Polyimides, in Kirk-Othmer Encyclopedia of Chemical Technology; John Wiley & Sons: New York, 2006.
(32) Spitalsky, Z.; Tasis, D.; Papagelis, K.; Galiotis, C. *Prog. Polym. Sci.* **2010**, *35*, 357−401.
(33) Wang, S. R.; Zhang, Y.; Abidi, N.; Cabrales, L. *Langmuir* **2009**, *25*, 11078−11081.
(34) Zhang, X. Q.; Wan, S. H.; Pu, J. B.; Wang, L. P.; Liu, X. Q. *J. Mater. Chem.* **2011**, *21*, 12251−12258.
(35) Drake, K.; Mukherjee, I.; Mirza, K.; Ji, H. F.; Wei, Y. *Macromolecules* **2011**, *44*, 4107−4115.
(36) Liu, Y. F.; Wang, Z.; Li, G.; Ding, M. X. *High Perform. Polym.* **2010**, *22*, 95−108.
(37) Zhang, X. F.; Liu, T.; Sreekumar, T. V.; Kumar, S.; Moore, V. C.; Hauge, R. H.; Smalley, R. E. *Nano Lett.* **2003**, *3*, 1285−1288.
(38) Zhao, X.; Zhang, Q. H.; Chen, D. J. *Macromolecules* **2010**, *43*, 2357−2363.
(39) Yang, Y.; Ren, L. L.; Zhang, C.; Huang, S.; Liu, T. X. *ACS Appl. Mater. Interfaces* **2011**, *3*, 2779−2785.
(40) Sun, H. J.; Huo, H. T.; Hao, N.; Yang, S. Y.; Lin, F. *Eur. Polym. J.* **2009**, *45*, 1169−1178.
(41) Zhang, L. M.; Lu, Z. X.; Zhao, Q. H.; Huang, J.; Shen, H.; Zhang, Z. J. *Small* **2011**, *7*, 460−464.
(42) Satti, A.; Larpent, P.; Gun'ko, Y. *Carbon* **2010**, *48*, 3376−3381.
(43) Cao, Y. W.; Feng, J. C.; Wu, P. Y. *Carbon* **2010**, *48*, 1683−1685.
(44) Paredes, J. I.; Villar-Rodil, S.; Martinez-Alonso, A.; Tascón, J. M. D. *Langmuir* **2008**, *24*, 10560−10564.
(45) Li, W. J.; Tang, X. Z.; Zhang, H. B.; Jiang, Z. G.; Yu, Z. Z.; Du, X. S.; Mai, Y. W. *Carbon* **2011**, *49*, 4724−4730.
(46) Liang, J. J.; Huang, Y.; Zhang, L.; Wang, Y.; Ma, Y. F.; Guo, T. Y.; Chen, Y. S. *Adv. Funct. Mater.* **2009**, *19*, 2297−2302.
(47) Ramanathan, T.; Abdala, A. A.; Stankovich, S.; Dikin, D. A.; Herrera-Alonso, M.; Piner, R. D.; Adamson, D. H.; Schniepp, H. C.; Chen, X.; Ruoff, R. S.; Nguyen, S. T.; Aksay, I. A.; Prud'homme, R. K.; Brinson, L. C. *Nat. Nanotechnol.* **2008**, *3*, 327.
(48) Tan, B.; Vasudevan, V.; Lee, Y. J.; Gardner, S.; Davis, R. M.; Bullions, T.; Loos, A. C.; Parvatareddy, H.; Dillard, D. A.; Mcgrath, J. E.; Cella, J. *J. Polym. Sci., Part A: Polym. Chem.* **1997**, *35*, 2943−2954.
(49) Yang, H. F.; Li, F. H.; Shan, C. S.; Han, D. X.; Zhang, Q. X.; Niu, L.; Lvaska, A. *J. Mater. Chem.* **2009**, *19*, 4632−4638.
(50) Feng, R. C.; Guan, G. H.; Zhou, W.; Li, C. C.; Zhang, D.; Xiao, Y. N. *J. Mater. Chem.* **2011**, *21*, 3931−3939.
(51) Cho, D.; Lee, S.; Yang, G.; Fukushima, H.; Drzal, L. T. *Macromol. Mater. Eng.* **2005**, *290*, 179−187.
(52) Gomez-Navarro, C.; Burghard, M.; Kern, K. *Nano Lett.* **2008**, *8*, 2045−2049.
(53) Zheng, X.; Ke, S. H.; Yang, W. T. *J. Chem. Phys.* **2010**, *132*, 114703.
(54) Meyer, F.; Minoia, A.; Raquez, J. M.; Spasova, M.; Lazzaroni, R.; Dubois, P. *J. Mater. Chem.* **2010**, *20*, 6873−6880.
(55) Yuen, S. M.; Ma, C. C.; Lin, Y. Y.; Kuan, H. C. *Compos. Sci. Technol.* **2007**, *67*, 2564−2573.
(56) Yang, X. M.; Li, L.; Shang, S. M.; Tao, X. M. *Polymer* **2010**, *51*, 3431−3435.
(57) Fang, M.; Zhang, Z.; Li, J. F.; Zhang, H. D.; Lu, H. B.; Yang, Y. L. *J. Mater. Chem.* **2010**, *20*, 9635−9643.
(58) Cai, D. Y.; Song, M. *J. Mater. Chem.* **2010**, *20*, 7906−7915.
(59) McLauchlin, A. R.; Thomas, N. L. *Polym. Degrad. Stab.* **2009**, *94*, 868−872.